

QRS Complex Detection in ECG Signals Using Empirical Wavelet Transform and Flower Pollination Algorithm

Fatima Guendouzi^{1*}, Mokhtar Attari¹

¹ Laboratory of Instrumentation (LINS), Faculty of Electrical Engineering, University of Science and Technology Houari Boumediene (USTHB), P. O. B. 32, Bab-Ezzouar 16111, Algeria

* Corresponding author, e-mail: fguendouzi@usthb.dz

Received: 27 May 2022, Accepted: 06 September 2022, Published online: 22 September 2022

Abstract

The QRS complex is the most important component of electrocardiogram (ECG) signals; therefore, its detection is the first step of all kinds of automatic feature extraction and crucial part of an ECG analysis system. The R wave is one of the most important sections of the QRS complex, which has an essential role in diagnosis of irregular heartbeats. This paper employs Empirical Wavelet Transform (EWT) and Hilbert transforms as well as by employing Flower Pollination Algorithm (FPA) in order to approach an optimum combinational method for R peak detection. First, the Empirical Wavelet Transform (EWT) is used to eliminate the noise and improve the envelope extraction. The Hilbert envelope is then used to determine the positions of the R waves. Finally, FPA is used to adjust the envelope's parameters. In the experimental section of this paper, the proposed approach is evaluated using the MIT/BIH database. We show that the proposed method can achieve results that are comparable to the state-of-the-art, with a global sensitivity of 99.95%, a positive predictivity of 99.92%, and a percentage error of 0.136%.

Keywords

Empirical Wavelet Transform (EWT), ECG, R peak, Hilbert transform, Flower Pollination Algorithm (FPA)

1 Introduction

Electrocardiography (ECG) is by far the most frequently used diagnostic tool. Therefore, a large number of scientists have attempted to develop automatic algorithms to help medical staff in making fast and accurate decisions. The two major fields of ECG analysis are QRS waveform detection and arrhythmia classification.

The QRS complexes serve as reference points for the automatic heart rate detection analysis and feature extraction. For many years, QRS complex detection has been a research topic. Numerous new approaches have been proposed in the literature, to be extensively reviewed; see [1]. The slope of the R wave is a popular signal feature used to locate the QRS complex in many QRS detectors. Such algorithms are based on signal derivatives [2–4]. However, this algorithm based on drives does not guarantee the detection of R peaks with large complex QRS because of ventricular anomalies such as extrasystoles.

Other algorithms based on more sophisticated digital filters and irregular RR interval checkup strategies are published in [5]. New algorithms based on artificial neural networks [6, 7]. However, due to the presence of noise and

anomalies and the time-varying form of the QRS complex, the early real-time algorithms showed poor accuracy.

To improve the algorithm for correct ECG wave extraction, various methods have been used [8–20]. Belkadi and Daamouche [8] proposed a new technique using a Particle Swarm Optimization (PSO) algorithm to look for the best values of the parameters of the popular Pan-Tompkins algorithm. Kozia et al. [9] presented an empirical mode decomposition-based algorithm for QRS complex detection, it uses an adaptive threshold over a sliding window combined with a gradient-based and refractory period checks to differentiate large Q peaks and reject false R peaks.

Several other techniques for R-peak detection have also been reported in various studies. These include mathematical morphology [10, 11], quadratic filter [12], filter banks [13], neural network [14–16], weighted total variation denoising [17], Hilbert transform [18], max-min difference algorithm [19].

To solve the problem of specific battement forms, several authors have used wavelet transform and multiresolution

analysis to account for the differences in the frequency of normal and pathological battements [20–29]. Li et al. [20] described a wavelet-based QRS detection algorithm by searching for the maximum modulus of wavelet coefficients greater than the update threshold. In [21], a new method for detecting ECG waves using the Daubechies wavelet function is described. The author developed and evaluated an ECG feature extraction system based on a multiresolution wavelet transform. This method achieves a sensitivity of 99.18% and a positive prediction rate of 98%. The author in [22] explained multiresolution analysis using a binary wavelet transform. The potential advantages of signal decomposition under different time scales will be realized, and therefore, different special resolutions will be realized. In addition, certain types of noise and baseline drift can be removed from the original signal according to the corresponding frequency range of the original signal so that the detection algorithm has good performance [23, 24]. Pal and Mitra [24] proposed an ECG wave detection system based on a multiresolution wavelet transform. They used a selective coefficient method based on the identification of the appropriate and optimal set of wavelet coefficients to reconstruct the wave or complex of interest from the ECG record. The R peak detection algorithm is verified on the PTB diagnostic database, and its accuracy is 99%. Jeong et al. [25] proposed a QRS detection processor using a quadratic spline wavelet transform for wireless ECG acquisition. The algorithm proposed by Zidelmal et al. [26] is based on wavelet detail coefficients to detect R-wave positions in signals with multiple QRS morphologies. Their method is based on the power spectrum of QRS complexes at different energy levels, including normal and pathological levels. The algorithm uses the entire MIT-BIH record for evaluation, and its sensitivity is 99.64%, the positive prediction rate is 99.82%, and the error rate is 0.54%. However, some records with deformed QRS shapes, artifacts, and baseline shifts (105, 108, 201, 203, and 228) have high error rates. A wavelet filter bank-based R-peak detector for a low-power cardiac pacemaker is described in [27]. Discrete wavelets transform (Daubechies db10 wavelet)-based R-peak detector is described in [28]. Modak et al. [29] presented a new technique for detecting QRS using DWT, median filtering, with adaptive multilevel thresholding (AMT). The wavelet transform-based peak finding logics are efficient, but for the selection of the mother wavelet, there is no general rule, and the performance of the wavelet transform-based algorithm depends on the application [28].

The robustness and high accuracy of detecting R peaks in ECG signals still remain open issues. This paper tries to benefit from the advantages of Hilbert and the Empirical Wavelet Transforms (EWT) as well as Flower Pollination Algorithm (FPA) in order to approach an optimum combinational method for R peak detection. To achieve this, we propose the EWT to filter the signal. The positions of the R waves are then detected using the Hilbert envelope from the de-noised signal. Finally, the FPA is used in order to find the best envelope threshold values; we formulate the parameter design as an optimization problem using three objective functions namely, maximum positive predictivity (P^+), maximum sensitivity (S_e), and minimum error rate (E_r). The proposed method is implemented according to the weighted-sum approach to combine multi-objectives into a composite one objective function. Specifically, the method combines EWT, Hilbert transform, and FPA is used for the first time in R peak detection. In addition FPA is an intelligent optimization algorithm that adopts the Lévy flight mechanism and uses a parameter to convert between a local search and a global search. Compared with similar algorithms, it has fewer parameters, is simple and easy to adjust, and is widely used in multi-objective function optimization.

The remainder of this paper is organized as follows. In Section 2, we give a brief theory about the Empirical Wavelet Transform (EWT), and we describe the details of the proposed method. Section 3 is dedicated to the obtained results and their discussion. Finally, Section 4 concludes our study.

2 QRS detection algorithm

2.1 MIT-BIH Arrhythmia Database

The data provided by the MIT-BIH Arrhythmia Database are a standard used by many researchers. The MIT-BIH Arrhythmia Database has 48 records. Each record has a 30 min sampling frequency of 360 Hz and an 11-bit resolution over a 10 mV range. Each record was independently annotated by two cardiologists or more to obtain computer-readable reference annotations for all beats contained in the database (approximately 110,000 annotations in total). Since the database was made public [30, 31], the annotations have been revised many times.

2.2 Empirical Wavelet Transform (EWT)

Gilles introduced the Empirical Wavelet Transform (EWT) in 2013. EWT is a novel approach to build wavelets adapted to represent the processed signal. The adaptability

of EWT is because filters' supports depend on where the information in the analyzed signal.

The detailed calculation process of EWT was introduced in [32]. The EWT process contains two important aspects:

1. segmenting the spectrum of the signal: detect the local maxima ω_n in the spectrum and select the top M values in descending order as MA . The first largest maxima are kept to form a peak sequence. The boundaries of all segments are defined as the center of two consecutive local maxima values.
2. Empirical wavelets are constructed and applied to process each segment of the signal.

$$\phi_n(\omega) = \begin{cases} 1 & \text{if } |\omega| \leq \omega_n - \tau_n \\ \cos\left[\frac{\pi}{2} \nu\left(\frac{1}{2\tau_n}(|\omega| - \omega_n + \tau_n)\right)\right] & \text{if } \omega_n - \tau_n \leq |\omega| \leq \omega_n + \tau_n \\ 0 & \text{otherwise} \end{cases} \quad (1)$$

$$\psi_n(\omega) = \begin{cases} 1 & \text{if } \omega_n + \tau_n \leq |\omega| \leq \omega_{n+1} - \tau_{n+1} \\ \cos\left[\frac{\pi}{2} \nu\left(\frac{1}{2\tau_{n+1}}(|\omega| - \omega_{n+1} + \tau_{n+1})\right)\right] & \text{if } \omega_{n+1} - \tau_{n+1} \leq |\omega| \leq \omega_{n+1} + \tau_{n+1} \\ \sin\left[\frac{\pi}{2} \nu\left(\frac{1}{2\tau_n}(|\omega| - \omega_n + \tau_n)\right)\right] & \text{if } \omega_n - \tau_n \leq |\omega| \leq \omega_n + \tau_n \\ 0 & \text{otherwise} \end{cases} \quad (2)$$

A properly selected parameter τ_n guarantees that EWT is a tight frame. The $\nu(x)$ is the auxiliary function of the Meyer wavelet defined as follows [32]:

$$\nu(x) = \begin{cases} x^4(35 - 84x + 70x^2 - 20x^3) & \text{if } 0 < x < 1 \\ 0 & \text{otherwise} \end{cases} \quad (3)$$

An example of a spectrum segmentation of an empirical filter bank for $\omega_1 = 1.5$ rad/s, $\omega_2 = 2$ rad/s, $\omega_3 = 2.8$ rad/s is given in Fig. 1.

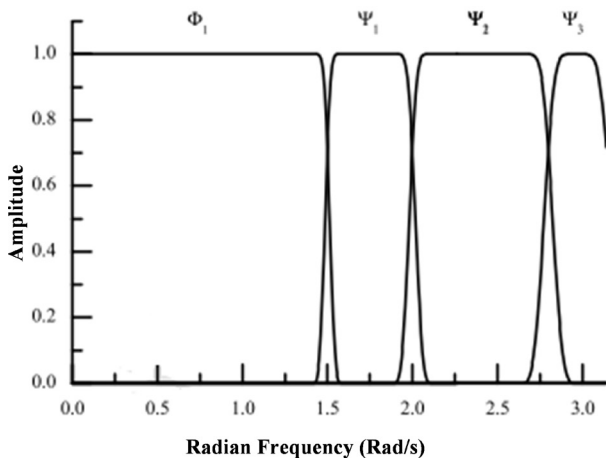


Fig. 1 Example of a spectrum segmentation of an empirical filter bank

The spectrum restricted to a range of $0 \sim \pi$ is divided into N contiguous segments. The boundaries of all segments are denoted by ω_n (where $\omega_0 = 0$ and $\omega_N = \pi$).

Therefore, each segment is defined as $\Lambda_n = [\omega_{n-1}, \omega_n]$. It is obvious that $\bigcup_{n=1}^N \Lambda_n = [0, \pi]$. A transient phase whose width is $2\tau_n$ is defined around each ω_n .

Based on the detected spectral boundaries, we choose the Meyer wavelet as the basis function [32]. The corresponding scaling function and empirical wavelets of EWT are designed by using Eqs. (1) and (2), respectively:

Define EWT after exporting the scaling function and the empirical wavelet. The approximated coefficients are the inner product of the signal and the scaling function:

$$W_f^e(0, t) = \langle f, \varnothing_1 \rangle = \int f(\tau) \overline{\varnothing_1(\tau - 1)} d\tau \quad (4)$$

The detail coefficients are the inner product of the signal, and the empirical wavelets are given by

$$W_f^e(n, t) = \langle f, \psi_n \rangle = \int f(\tau) \overline{\psi_n(\tau - 1)} d\tau \quad (5)$$

Then, the empirical modes decomposed from the signal are presented below:

$$f_0(t) = W_f^e(0, t) * \varnothing_1(t) \quad (6)$$

$$f_k(t) = W_f^e(n, t) * \psi_k(t) \quad (7)$$

In this case, the number of modes $N = 10$, for a standard ECG signal 234 with 1800 samples (5 s), sampled at a frequency of 360 Hz, along with ten modes decomposed by EWT, as shown in Fig. 2.

The flowchart diagram of the proposed R peak detection method is shown in Fig. 3. First, we used an Empirical Wavelet Transform (EWT) for ECG enhancement from

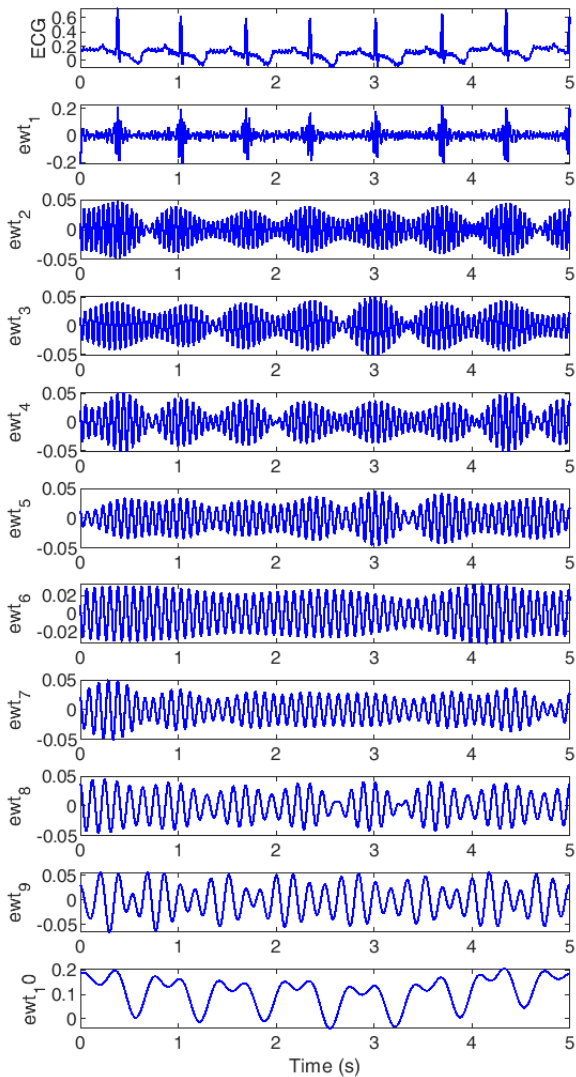


Fig. 2 Decomposition of the original signal 234 m using EWT

high- and low-frequency noise. The signal is processed by the EWT to build wavelets adapted to represent the processed signal. The spectrum of the detail coefficient is studied to select where the energy of the signal is concentrated. When EWT is applied to the noisy signal, the estimate of powerline interference is provided by the last mode (ewt10); however, the baseline is estimated by the

first mode (ewt1). Hence, removing these modes from the noisy ECG signal provides the denoised ECG. Then, a Hilbert envelope is applied to the resulting signal to determine the positions of the R waves. Finally, FPA is used to adjust the envelope's parameters. We define in each beat a window of 160 ms (57 samples) duration. Each window starts from the first determined point that satisfies the threshold condition.

The power spectrum of the detail coefficient is calculated based on the Fast Fourier Transform (FFT). The energy content of the decomposed signal is shown in Fig. 4.

When EWT is applied to a noisy signal, the estimate of powerline interference is provided by the last mode (ewt10). However, the baseline is estimated by the first mode (ewt1). Hence, removing these modes from the noisy ECG signal provides the denoised ECG.

The energy of the QRS complex is concentrated within the frequency range (5–22 Hz) for normal and abnormal beats, as shown in [25]. Hence, it is evident from Fig. 4 that the energy of the signal under investigation is concentrated at detail coefficients ewt3, ewt4, ewt5 and ewt6, having the frequency ranges (11.25–22.5 Hz) and (5.62–11.25 Hz), respectively.

Fig. 5 shows the typical representation of the original and the free noise signal for the segment (0–5 s) of the ECG record 234 m. It is evident that the baseline wander existing in the segment is corrected and the high-frequency noise is well eliminated.

2.3 Hilbert transform

The Hilbert transform was introduced in the early 20th century by David Hilbert and is widely used in signal theory to describe the complex envelope of a full scale modulated by a signal. Given a real-time function $x(t)$, its Hilbert transform is defined as:

$$\hat{x}(t) = H[x(t)] = x(t) * \frac{1}{\pi t} = \frac{1}{\pi} \int_{-\infty}^{+\infty} \frac{x(\tau)}{t - \tau} d\tau, \quad (8)$$

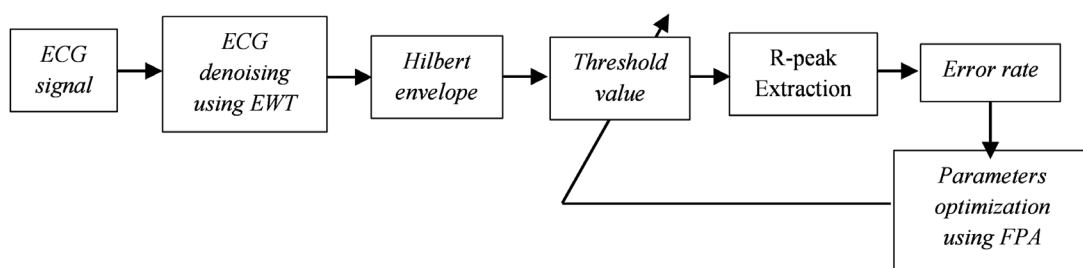


Fig. 3 Flowchart showing the steps involved in the proposed optimization scheme

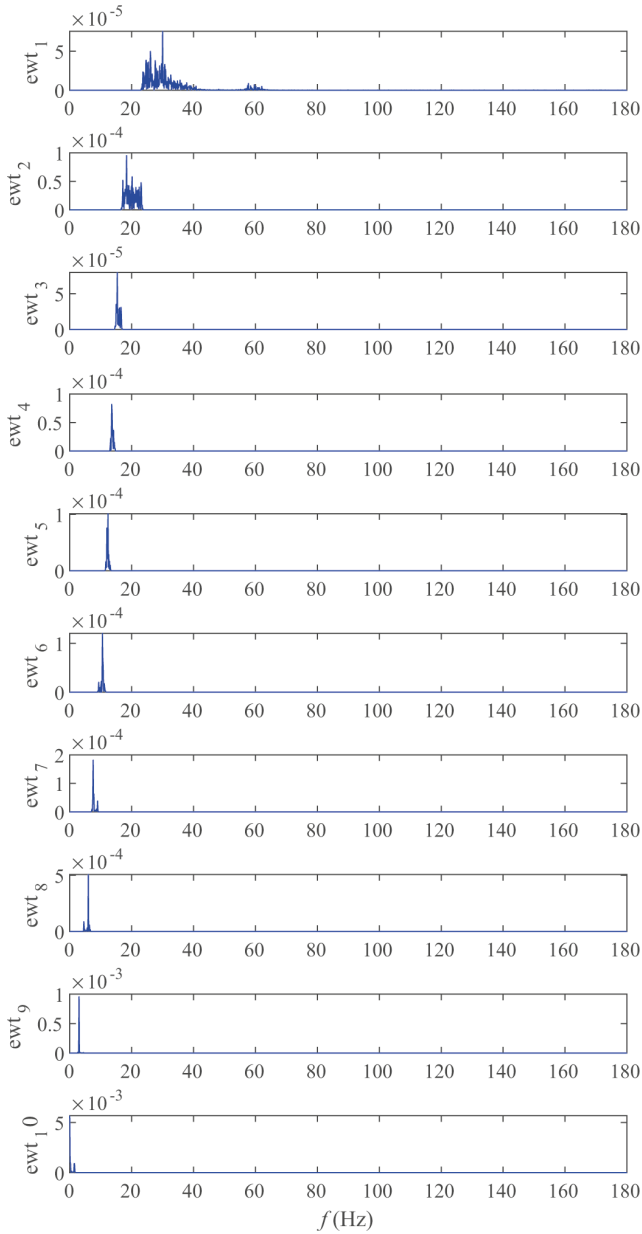


Fig. 4 Power spectrum of the denoised signal

$x(t)$ and $\hat{x}(t)$ are correlated to each other in such a manner that they together create a strong analytic signal. The analytic signal is expressed as:

$$x_a(t) = x(t) + iH[x(t)].$$

The module of the analytic signal provides the Hilbert envelope of $x(t)$, which is defined as:

$$B(t) = \sqrt{x(t)^2 + H[x(t)]^2}. \tag{9}$$

The envelope determined using Eq. (9) will have the identical slope and magnitude of the original signal $x(t)$.

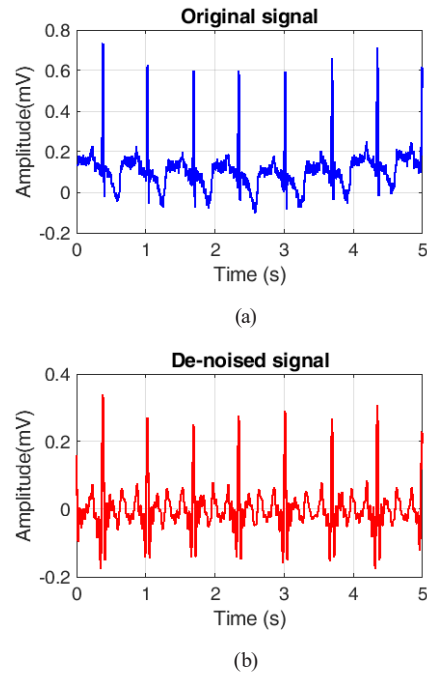


Fig. 5 (a) Original ECG signal 234 m for 1800 samples.
 (b) Denoised signal

2.4 Extraction of R-peak positions

Fig. 2 shows the flowchart of the R-peak detection algorithm, which can be summarized as follows:

1. Apply EWT to the noisy ECG signal $x(i)$,
2. Compute the Hilbert envelope $B(i)$,
3. QRS localization: select $B(i)$ associated to QRS complex using a threshold $TH = \lambda * \max(B)$,
4. Then, we search the beginning of the window. Each window starts from the first determined point which satisfies the threshold condition.
 - if $B(i) \geq TH$ then position $i \Rightarrow$ QRS (candidate),
 - else position $i \Rightarrow$ Not QRS.
5. Since the maximum duration of QRS complex is <160 ms, we define in each beat a window of 160 ms (57 samples) duration.
6. The R peaks positions are identified as the points with the maximum amplitude of the signal ECG denoising in each predefined window.
7. Elimination of multiple detection: The refractory period of 200 ms (72 samples) between two consecutive searches is regarded [2]. This constraint is a physiological one due to the refractory period during which ventricular depolarization cannot occur.

The indexes corresponding to the various detected positions are stored in a new array, named R peaks, and they are represented in Figs. 6 and 7.

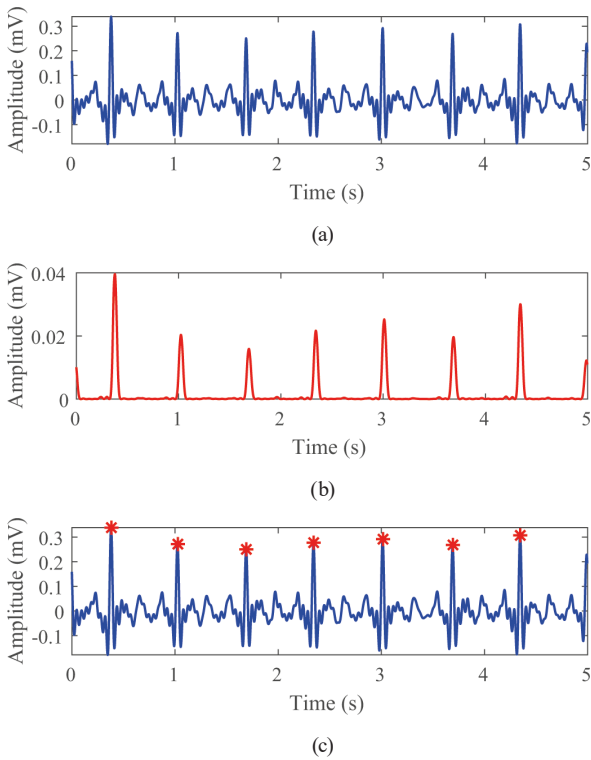


Fig. 6 Representation of the (a) original signal 234 m, (b) improved approximate envelope and (c) R peak positions

2.5 Optimization with the Flower Pollination Algorithm

The Flower Pollination Algorithm (FPA), developed by Xin-She Yang in 2012 [33], was inspired by the flow pollination process of flowering plants. The flower pollination process aims to transfer pollen between the same or diverse plant species for reproductive purposes. The FPA has been extended to multi-objective optimization [34]. For simplicity, the following four rules are used:

1. global pollination process, both biotic and cross-pollination steps can be realized by performing Lévy flights.
2. local pollination includes abiotic and self-pollination.
3. the reproduction possibility is proportional to the resemblance between any two flowers.
4. the switch probability $p \in [0,1]$ can be controlled between local and global pollination. Due to certain external factors (e.g., wind), local pollination includes an important portion of all pollination activities.

The main rules can be summarized in the pseudocode of the FPA implemented in Algorithm 1, where $\epsilon \in \Re$ denotes a small amount of value.

3 Results and discussions

In Section 3, the performance of the proposed QRS complex detection method was evaluated using ECG signals

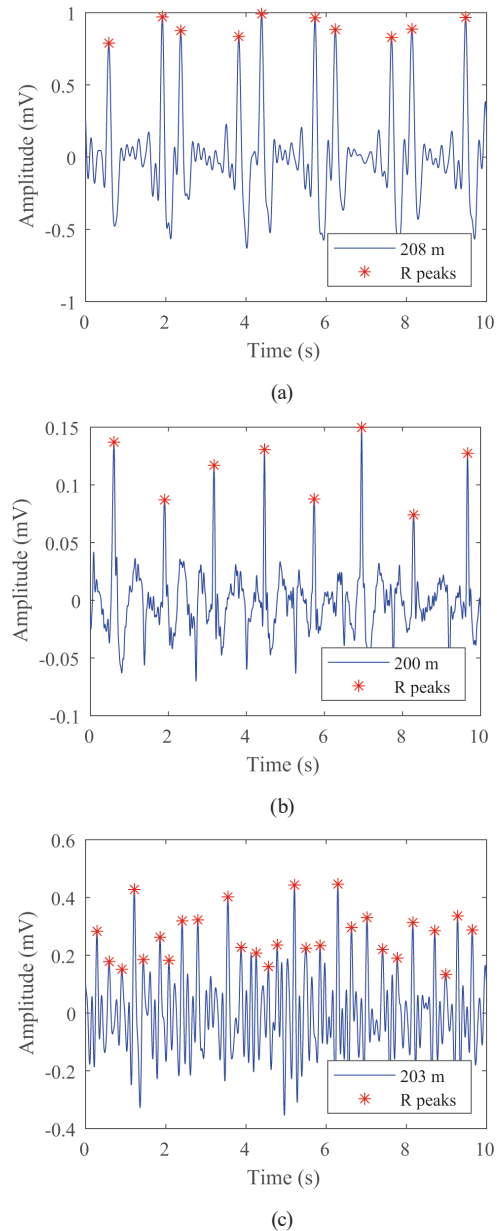


Fig. 7 Results of R peak detection for segments from MIT-BIH records: (a) Record 208, (b) Record 200, (c) Record 203

from the MIT-BIH database; all 48 arrhythmia ECG signals from MIT-BIH were taken.

In this study, a multi-objective Flower Pollination Algorithm (FPA) with EWT and Hilbert envelope is proposed to solve the QRS complex detection problem. The novelty of this study is to find the best threshold values of the envelope using the Flower Pollination Algorithm (FPA) based on three measurement criteria for QRS complex detection, namely, maximum positive predictivity (P^+), maximum sensitivity (S_e), and minimum error rate (E_r). All three measurements can be calculated using Eqs. (10)–(12):

Algorithm 1 Flower Pollination Algorithm pseudocode

```

1: Objective:  $\min f(\mathbf{x}), \mathbf{x} \in \mathfrak{R}^d$ 
2: Initialize a population of  $n$  flowers (pollens) with random solutions.
3: Find the best solution  $\mathbf{x}^*$  in the initial population.
4: Define a switch probability  $p \in [0,1]$ .
5: Calculate all  $f(\mathbf{x})$  for  $n$  solutions.
6:  $t = 0$ 
7: while  $t \leq \text{MaxGeneration}$  do
8:     for  $i = 1, \dots, n$  do
9:          $\text{rnd} \leftarrow U(0,1)$ .
10:        if  $\text{rnd} \leq p$  then
11:            Draw a  $d$ -dimensional step vector  $\xi$  which obeys a Lévy distribution.
12:            Perform global pollination via  $\mathbf{x}_i^{t+1} = \mathbf{x}_i^t + \xi * (\mathbf{g}^* - \mathbf{x}_i^t)$ .
13:        else
14:            Draw from a uniform distribution  $U(0,1)$ .
15:            Randomly choose  $j$  and  $k$  among all solutions, such that  $j \neq k$ .
16:            Perform local pollination via  $\mathbf{x}_i^{t+1} = \mathbf{x}_i^t + \epsilon (\mathbf{x}_j^t - \mathbf{x}_k^t)$ .
17:        end if
18:        Calculate  $f(\mathbf{x}')$ .
19:        if  $f(\mathbf{x}') \leq f(\mathbf{x})$  then
20:             $\mathbf{x} \leftarrow \mathbf{x}'$ .
21:        end if
22:    end for
23:    Find the current best solution  $\mathbf{x}^*$  among all  $\mathbf{x}_i^t$ .
24:     $t = t + 1$ .
25: end while
    
```

$$P^+ (\%) = \left[\frac{TP}{TP + FP} \right] \times 100 \tag{10}$$

$$S_e (\%) = \left[\frac{TP}{TP + FN} \right] \times 100 \tag{11}$$

$$E_r (\%) = \left[\frac{FP + FN}{TB} \right] \times 100 \tag{12}$$

where:

TP: number of true positives indicates the accurate detection of R peaks.

FN: number of false negatives, representing the failure of the algorithm to detect a real beat.

FP: number of false positives indicating the erroneous detections of R peaks.

TB: total analyzed beat.

Positive predictivity (P^+) is the probability that classified beat as true beat, i.e., positive predictivity reports the percentage of beat detections, which is true, beats.

Sensitivity is the capability to detect true beats, i.e., sensitivity indicates the percentage of true beats that are correctly detected by the algorithm. The error rate is

approximately two types of errors, false positives and false negatives, and the sum of *FP* and *FN* is the total error.

The testing results are given in Table 1 for all records from the first channel of the MIT-BIH database. We obtained a global sensitivity (S_e) and positive predictivity (P^+) of 99.95 and 99.92%, respectively. The error rate of R peak detection for all analyzed beats is 0.136%. Table 2 summarizes the comparison of the proposed algorithm with other algorithms found in the literature. It is evident that our algorithm presents good accuracy because it gives comparable test parameters with some works and the highest parameters to others.

The achieved results reported in Table 1 show statistical indices higher than or comparable to those cited in literature (see Table 2). The obtained results show 99.95% sensitivity, a 99.92% positive predictivity, and a detection error rate of only 0.136. The proposed method is then compared to ten other state-of-the-art methods, and it outperforms eight of them in all aspects (see Table 2). Even if the Nayak et al. [11] method has higher positive predictivity than the proposed algorithm, the difference is negligible. The proposed method has far greater positive

Table 1 Experimental results of the R peak detection algorithm

Record	<i>T_B</i>	<i>T_P</i>	<i>FP</i>	<i>FN</i>	<i>S_e</i> (%)	<i>P_r</i> (%)	<i>E_r</i> (%)
100	2273	2273	0	0	100	100	0
101	1865	1865	0	0	100	100	0
102	2187	2184	0	3	99.86	100	0.137
103	2084	2084	0	0	100	100	0
104	2229	2226	1	3	99.86	99.95	0.179
105	2572	2569	15	3	99.88	99.42	0.699
106	2027	2027	0	0	100	100	0
107	2137	2137	0	0	100	100	0
108	1763	1757	0	6	99.6597	100	0.340
109	2532	2532	0	0	100	100	0
111	2124	2123	1	1	99.95	99.95	0.094
112	2539	2539	0	0	100	100	0
113	1795	1795	1	0	100	99.94	0.056
114	1879	1874	1	5	99.73	99.95	0.319
115	1953	1953	0	0	100	100	0
116	2412	2412	0	0	100	100	0
117	1535	1535	0	0	100	100	0
118	2278	2277	1	1	99.96	99.96	0.088
119	1987	1986	0	1	99.95	100	0.050
121	1863	1863	1	0	100	99.95	0.054
122	2476	2476	0	0	100	100	0
123	1518	1518	0	0	100	100	0
124	1619	1618	1	1	99.94	99.94	0.123
200	2601	2600	2	1	99.96	99.92	0.115
201	1963	1960	6	3	99.85	99.69	0.458
202	2136	2134	0	2	99.91	100	0.094
203	2980	2977	16	3	99.90	99.46	0.638
205	2656	2656	7	0	100	99.74	0.264
207	1860	1858	9	2	99.89	99.52	0.591
208	2955	2951	10	4	99.86	99.66	0.474
209	3005	3005	0	0	100	100	0
210	2650	2644	2	6	99.77	99.92	0.302
212	2748	2748	0	0	100	100	0
213	3251	3251	1	0	100	99.97	0.031
214	2262	2262	2	0	100	99.91	0.088
215	3363	3363	0	0	100	100	0
217	2208	2208	1	0	100	99.95	0.045
219	2154	2154	0	0	100	100	0
220	2048	2048	0	0	100	100	0
221	2427	2426	1	1	99.96	99.96	0.082
222	2483	2480	6	3	99.88	99.76	0.362
223	2605	2605	0	0	100	100	0
228	2053	2048	7	5	99.76	99.66	0.584
230	2256	2256	0	0	100	100	0
231	1571	1571	0	0	100	100	0
232	1780	1778	2	2	99.89	99.89	0.225
233	3079	3079	0	0	100	100	0
234	2753	2753	1	0	100	99.96	0.036
All	109494	109438	95	56	99.95	99.92	0.136

Table 2 Comparison with other algorithms

Method	TP	FP	FN	S_e (%)	P^+ (%)	E_r (%)
Presented algorithm	109438	95	56	99.95	99.92	0.136
Banerjee et al. [23]	19022	76	40	99.60	99.50	0.61
Zidelmal et al. [26]	109101	193	393	99.64	99.82	0.54
Afonso et al. [13]	90535	406	374	99.59	99.56	0.86
Pan and Tompkins [2]	109532	507	277	99.75	99.54	0.71
Hamilton and Tompkins [3]	108927	248	340	99.69	99.77	0.54
Li et al. [20]	104070	65	112	99.89	99.94	0.17
Nayak et al. [11]	109494	70	52	99.95	99.94	0.11
Jia et al. [16]	109494	-	-	99.89	99.90	0.21
Pandit et al. [19]	109432	369	389	99.65	99.66	-
Modak et al. [29]	109494	130	289	99.74	99.88	0.38

predictivity and a lower detection error rate than [2, 3, 13, 16, 19, 20, 23, 26, 29].

Fig. 6 (a) shows a section from record 234 of the MIT-BIH arrhythmia database. Fig. 6 (b) represents the improved approximate envelope, while Fig. 5 (c) shows the R peak position.

Fig. 7 illustrates some ECG segments with complicated patterns to demonstrate the effectiveness of R peak localization. Fig. 7 (a) captures the position of R peaks on a section of record 208 that contains PVC-corresponding beats. The R peaks are well localized. Fig. 7 (b) represents a segment of record 200. A special case of PVCs beats is shown, called Bigminy, where premature ventricular beats occur in an alternating pattern after every normal beat. All normal and abnormal QRS beats are detected successfully.

Fig. 7 (c) depicts the position of R peaks on a section from record 203. Record 203 contains ectopic beats with variable RR intervals and R amplitude variation. The positions of the R peaks are correctly detected.

The QRS detection algorithm was applied to the entire data of the MIT-BIH database from lead I. It presents the possibility of detecting R locations of great variations of normal and abnormal QRS complexes with the influence of different kinds of cardiac arrhythmias.

References

- [1] Köhler, B.-U., Hennig, C., Orglmeister, R. "The principles of software QRS detection", IEEE Engineering in Medicine and Biology Magazine, 21(1), pp. 42–57, 2002.
<https://doi.org/10.1109/51.993193>
- [2] Pan, J., Tompkins, W. J. "A real-time QRS detection algorithm", IEEE Transactions on Biomedical Engineering, BME-32(3), pp. 230–236, 1985.
<https://doi.org/10.1109/TBME.1985.325532>

4 Conclusion

In this paper, we presented a novel approach for R peak detection in the ECG signal using Hilbert and Empirical Wavelet Transforms, as well as a Flower Pollination Algorithm (FPA). The EWT is used to denoise the ECG signal; the last mode (ewt10) estimates powerline interference; however, the first mode estimates the baseline (ewt1). Hence, removing these modes from the noisy ECG signal yields the denoised ECG. The positions of the R waves are then detected using the Hilbert envelope from the resulting signal. Though the FPA has fewer parameters, is simple and easy to adjust, and it is widely used in multi-objective function optimization. It allowed us to find an optimal value of the envelope threshold to minimize the number of the false detection. The QRS detection algorithm was applied to the entire data of the MIT-BIH database from lead I. According to our results, combination of EWT, Hilbert transform, and FPA has a significant effect in the detection of R wave and outperforms the others. It offers the possibility of detecting R locations with great variations in both normal and pathological QRS complexes.

In perspective, an ECG heartbeats classifier can be provided to classify and categorize various QRS complex anomalies (e.g., PVCs, APCs, LBBBs, and RBBBs beats).

- [3] Hamilton, P. S., Tompkins, W. J. "Quantitative investigation of QRS detection rule using the MIT/BIH arrhythmia database", *IEEE Transactions on Biomedical Engineering*, BME-33(12), pp. 1157–1165, 1986.
<https://doi.org/10.1109/TBME.1986.325695>
- [4] Banerjee, S. "A first derivative based R-peak detection and DWT based beat delineation approach of single lead electrocardiogram signal", In: 2019 IEEE Region 10 Symposium (TENSYP), Kolkata, India, 2019. pp. 565–570. ISBN 978-1-7281-0298-6
<https://doi.org/10.1109/TENSYP46218.2019.8971094>
- [5] Choi, S., Adnane, M., Lee, G.-J., Jang, H., Jiang, Z., Park, H.-K. "Development of ECG beat segmentation method by combining low pass filter and irregular R-R interval checkup strategy", *Expert Systems with Applications*, 37(7), pp. 5208–5218, 2010.
<https://doi.org/10.1016/j.eswa.2009.12.069>
- [6] Zhong, W., Liao, L., Guo, X., Wang, G. "A deep learning approach for fetal QRS complex detection", *Physiological Measurement*, 39(4), 045004, 2018.
<https://doi.org/10.1088/1361-6579/aab297>
- [7] Cai, W., Hu, D. "QRS complex detection using novel deep learning neural networks", *IEEE Access*, 8, pp. 97082–97089, 2020.
<https://doi.org/10.1109/ACCESS.2020.2997473>
- [8] Belkadi, M., Daamouche, A. "Swarm intelligence approach to QRS detection", *The International Arab Journal of Information Technology*, 17(4), pp. 480–487, 2020.
<https://doi.org/10.34028/iajit/17/4/6>
- [9] Kozia, C., Herzallah, R., Lowe, D. "ICA-Derived Respiration Using an Adaptive R-Peak Detector", In: Valenzuela, O., Rojas, F., Pomares, H., Rojas, I. (eds.) *Theory and Applications of Time Series Analysis: Selected Contributions from ITISE 2018*, Springer, 2019, pp. 363–377. ISBN 978-3-030-26035-4
https://doi.org/10.1007/978-3-030-26036-1_25
- [10] Nankani, D., Parabattina, B., Baruah, R. D., Das, P. K. "R-Peak Detection from ECG Signals Using Fractal Based Mathematical Morphological Operators", In: *TENCON 2021 - 2021 IEEE Region 10 Conference (TENCON)*, Auckland, New Zealand, 2021, pp. 225–230. ISBN 978-1-6654-9533-2
<https://doi.org/10.1109/TENCON54134.2021.9707247>
- [11] Nayak, C., Saha, S. K., Kar, R., Mandal, D. "An efficient and robust digital fractional order differentiator based ECG pre-processor design for QRS detection", *IEEE Transactions on Biomedical Circuits and Systems*, 13(4), pp. 682–696, 2019.
<https://doi.org/10.1109/TBCAS.2019.2916676>
- [12] Phukpattaranont, P. "QRS detection algorithm based on the quadratic filter", *Expert Systems with Applications*, 42(11), pp. 4867–4877, 2015.
<https://doi.org/10.1016/j.eswa.2015.02.012>
- [13] Afonso, V. X., Tompkins, W. J., Nguyen, T. Q., Luo, S. "ECG beat detection using filter banks", *IEEE Transactions on Biomedical Engineering*, 46(2), pp. 192–201, 1999.
<https://doi.org/10.1109/10.740882>
- [14] Habib, A., Karmakar, C., Yearwood, J. "Learning post-processing for QRS detection using Recurrent Neural Network", [preprint] arXiv e-prints, arXiv:2110.04130 [eess.SP], 07 October 2021.
<https://doi.org/10.48550/arXiv.2110.04130>
- [15] Yuen, B., Dong, X., Lu, T. "Inter-patient CNN-LSTM for QRS complex detection in noisy ECG signals", *IEEE Access*, 7, pp. 169359–169370, 2019.
<https://doi.org/10.1109/ACCESS.2019.2955738>
- [16] Jia, M., Li, F., Wu, J., Chen, Z., Pu, Y. "Robust QRS detection using high-resolution wavelet packet decomposition and time-attention convolutional neural network", *IEEE Access*, 8, pp. 16979–16988, 2020.
<https://doi.org/10.1109/ACCESS.2020.2967775>
- [17] Sharma, T., Sharma, K. K. "QRS complex detection in ECG signals using locally adaptive weighted total variation denoising", *Computers in Biology and Medicine*, 87, pp. 187–199, 2017.
<https://doi.org/10.1016/j.combiomed.2017.05.027>
- [18] Manikandan, M. S., Soman, K. P. "A novel method for detecting R-peaks in electrocardiogram (ECG) signal", *Biomedical Signal Processing and Control*, 7(2), pp. 118–128, 2012.
<https://doi.org/10.1016/j.bspc.2011.03.004>
- [19] Pandit, D., Zhang, L., Liu, C., Chattopadhyay, S., Aslam, N., Lim, C. P. "A lightweight QRS detector for single lead ECG signals using a max-min difference algorithm", *Computer Methods and Programs in Biomedicine*, 144, pp. 61–75, 2017.
<https://doi.org/10.1016/j.cmpb.2017.02.028>
- [20] Li, C., Zheng, C., Tai, C. "Detection of ECG characteristic points using wavelet transforms", *IEEE Transactions on Biomedical Engineering*, 42(1), pp. 21–28, 1995.
<https://doi.org/10.1109/10.362922>
- [21] Mahmoodabadi, S. Z., Ahmadian, A., Abolhasani, M. D. "ECG feature extraction using daubechies wavelets", In: *Proceedings of the fifth IASTED International Conference on Visualization, Imaging and Image Processing*, Benidorm, Spain, 2005, pp. 343–348. ISBN 0-88986-528-0
- [22] Gautam, R., Sharma, A. K. "Detection of QRS complexes of ECG recording based on wavelet transform using Matlab", [pdf] *International Journal of Engineering Science and Technology*, 2(7), pp. 3038–3044, 2010. Available at: <http://www.ijest.info/docs/IJEST10-02-07-145.pdf> [Accessed: 27 May 2022]
- [23] Banerjee, S., Gupta, R., Mitra, M. "Delineation of ECG characteristic features using multiresolution wavelet analysis method", *Measurement*, 45(3), pp. 474–487, 2012.
<https://doi.org/10.1016/j.measurement.2011.10.025>
- [24] Pal, S., Mitra, M. "Detection of ECG characteristic points using multiresolution wavelet analysis based selective coefficient method", *Measurement*, 43(2), pp. 255–261, 2010.
<https://doi.org/10.1016/j.measurement.2009.10.004>
- [25] Jeong, C.-I., Mak, P.-I., Lam, C.-P., Dong, C., Vai, M.-I., Mak, P.-U., Pun, S.-H., Wan, F., Martins, R. P. "A 0.83- μ W QRS detection processor using quadratic spline wavelet transform for wireless ECG acquisition in 0.35- μ m CMOS", *IEEE Transactions on Biomedical Circuits and Systems*, 6(6), pp. 586–595, 2012.
<https://doi.org/10.1109/TBCAS.2012.2188798>
- [26] Zidelmal, Z., Amirou, A., Adnane, M., Belouchrani, A. "QRS detection based on wavelet coefficients", *Computer Methods and Programs in Biomedicine*, 107(3), pp. 490–496, 2012.
<https://doi.org/10.1016/j.cmpb.2011.12.004>

- [27] Min, Y.-J., Kim, H.-K., Kang, Y.-R., Kim, G.-S., Park, J., Kim, S.-W. "Design of wavelet-based ECG detector for implantable cardiac pacemakers", *IEEE Transactions on Biomedical Circuits and Systems*, 7(4), pp. 426–436, 2013.
<https://doi.org/10.1109/TBCAS.2012.2229463>
- [28] Rakshit, M., Das, S. "An efficient wavelet-based automated *R*-peaks detection method using Hilbert transform", *Biocybernetics and Biomedical Engineering*, 37(3), pp. 566–577, 2017.
<https://doi.org/10.1016/j.bbe.2017.02.002>
- [29] Modak, S., Taha, L. Y., Abdel-Raheem, E. "Single channel QRS detection using wavelet and median denoising with adaptive multilevel thresholding", In: *2020 IEEE International Symposium on Signal Processing and Information Technology (ISSPIT)*, Louisville, KY, USA, 2020, pp. 1–6. ISBN 978-1-6654-4683-9
<https://doi.org/10.1109/ISSPIT51521.2020.9408699>
- [30] Moody, G. B., Mark, R. G. "The impact of the MIT-BIH arrhythmia database", *IEEE Engineering in Medicine and Biology Magazine*, 20(3), pp. 45–50, 2001.
<https://doi.org/10.1109/51.932724>
- [31] Goldberger, A. L., Amaral, L. A. N., Glass, L., Hausdorff, J. M., Ivanov, P. C., Mark, R. G., Mietus, J. E., Moody, G. B., Peng, C.-K., Stanley, H. E. "PhysioBank, PhysioToolkit, and PhysioNet: Components of a new research resource for complex physiologic signals", *Circulation*, 101(23), pp. e215–e220, 2000.
<https://doi.org/10.1161/01.CIR.101.23.e215>
- [32] Gilles, J. "Empirical Wavelet Transform", *IEEE Transactions on Signal Processing*, 61(16), pp. 3999–4010, 2013.
<https://doi.org/10.1109/TSP.2013.2265222>
- [33] Yang, X.-S. "Flower pollination algorithm for global optimization", In: *Durand-Lose, J., Jonoska, N. (eds.) Unconventional Computation and Natural Computation*, Springer, 2012, pp. 240–249. ISBN 978-3-642-32893-0
https://doi.org/10.1007/978-3-642-32894-7_27
- [34] Yang, X.-S., Karamanoglu, M., He, X. "Multi-objective flower algorithm for optimization", *Procedia Computer Science*, 18, pp. 861–868, 2013.
<https://doi.org/10.1016/j.procs.2013.05.251>